Theoretical and Applied Genetics (2021) 134:3675–3686
https://doi.org/10.1007/s00122-021-03921-z

ORIGINAL ARTICLE

Oligo-FISH barcode in beans: a new chromosome identification system

Fernanda de Oliveira Bustamante[1,2] · Thiago Henrique do Nascimento[3] · Claudio Montenegro[3] · Sibelle Dias[1] · Lívia do Vale Martins[1,4] · Guilherme Tomaz Braz[5] · Ana Maria Benko-Iseppon[1] · Jiming Jiang[5,6] · Andrea Pedrosa-Harand[3] · Ana Christina Brasileiro-Vidal[1]

Received: 8 April 2021 / Accepted: 17 July 2021 / Published online: 8 August 2021

Abstract

Key message **An Oligo-FISH barcode system was developed for two model legumes, allowing the identification of all cowpea and common bean chromosomes in a single FISH experiment, and revealing new chromosome rearrangements. The FISH barcode system emerges as an effective tool to understand the chromosome evolution of economically important legumes and their related species.**

Abstract Current status on plant cytogenetic and cytogenomic research has allowed the selection and design of oligo-specific probes to individually identify each chromosome of the karyotype in a target species. Here, we developed the first chromosome identification system for legumes based on oligo-FISH barcode probes. We selected conserved genomic regions between *Vigna unguiculata* (*Vu*, cowpea) and *Phaseolus vulgaris* (*Pv,* common bean) (diverged ~ 9.7–15 Mya), using cowpea as a reference, to produce a unique barcode pattern for each species. We combined our oligo-FISH barcode pattern with a set of previously developed FISH probes based on BACs and ribosomal DNA sequences. In addition, we integrated our FISH maps with genome sequence data. Based on this integrated analysis, we confirmed two translocation events (involving chromosomes 1, 5, and 8; and chromosomes 2 and 3) between both species. The application of the oligo-based probes allowed us to demonstrate the participation of chromosome 5 in the translocation complex for the first time. Additionally, we detailed a pericentric inversion on chromosome 4 and identified a new paracentric inversion on chromosome 10. We also detected centromere repositioning associated with chromosomes 2, 3, 5, 7, and 9, confirming previous results for chromosomes 2 and 3. This first barcode system for legumes can be applied for karyotyping other Phaseolinae species, especially non-model, orphan crop species lacking genomic assemblies and cytogenetic maps, expanding our understanding of the chromosome evolution and genome organization of this economically important legume group.

Introduction

The development of a karyotype is essential to gain insights into the chromosome organization and evolution of related species. The early 1980s represented the beginning of the molecular cytogenetic era with the advent of FISH (Fluorescent In Situ Hybridization) technique (Langer-Safer et al. 1982). FISH provides a powerful tool for individual

Communicated by P. Heslop-Harrison.

Fernanda de Oliveira Bustamante and Thiago Henrique do Nascimento have contributed equally to this work.

✉ Andrea Pedrosa-Harand
andrea.harand@ufpe.br

✉ Ana Christina Brasileiro-Vidal
ana.vidal@ufpe.br

[1] Departamento de Genética, Universidade Federal de Pernambuco, Recife, PE, Brazil

[2] Present Address: Universidade do Estado de Minas Gerais, Unidade Divinópolis, Divinópolis, MG, Brazil

[3] Departamento de Botânica, Universidade Federal de Pernambuco, Recife, PE, Brazil

[4] Present Address: Departamento de Biologia, Universidade Federal do Piauí, Teresina, PI, Brazil

[5] Department of Plant Biology, Michigan State University, East Lansing, MI, USA

[6] Department of Horticulture, Michigan State University, East Lansing, MI 48824, USA

chromosome identification by using a wide range of DNA probes, including large-insert genomic DNA clones, such as BACs (Bacterial Artificial Chromosomes) (Jiang and Gill 1994, 2006; reviewed by Jiang 2019). Advances in sequencing technologies, with availability of genome sequences from an increasing number of species, and massive synthesis of oligonucleotides (oligos), have allowed the design of new probes for FISH, such as oligo-painting (Beliveau et al. 2012). These probes can be developed from any species with a sequenced and assembled genome and can be used in karyotype analyses of related species (Jiang 2019).

In plants, chromosome painting with oligo-based probes has been used to determine karyotypes and investigate chromosome rearrangements, meiotic pairing, and recombination in a wide range of species (Han et al. 2015; Qu et al. 2017; Braz et al. 2018, 2021; He et al. 2018, 2020; Hou et al. 2018; Meng et al. 2018; Xin et al. 2018; Albert et al. 2019; do Vale Martins et al. 2019; Šimoníková et al. 2019; Zhao et al. 2019; Bi et al. 2020; Bielski et al. 2020; Li et al. 2020; Liu et al. 2020; Piperidis and D'Hont 2020; Song et al. 2020). Oligos selected from multiple regions from multiple chromosomes can be used to produce a barcode signal pattern for an individual chromosome pair, allowing the identification of a complete set of individual chromosomes in a single FISH experiment (Braz et al. 2018). So far, the oligo-FISH barcode system has been established in a few species, including potato (Braz et al. 2018), maize (Braz et al. 2020a; 2021), rice (Liu et al. 2020), sugarcane (Meng et al. 2020; Piperidis and D'Hont 2020), *Ipomoea* taxa (Chen et al. 2020), and Triticeae tribe (Li et al. 2020).

Vigna Savi and *Phaseolus* L. (Leguminosae family, Phaseoloid clade, Phaseolinae subtribe) are phylogenetically related genera, which diverged about 9.7–15 million years ago (Mya) (Li et al. 2013; Garcia et al. 2020). The group includes socioeconomically important species, such as *Vigna unguiculata* (L.) Walp. (cowpea) and *Phaseolus vulgaris* L. (common bean), essential crops for global food security and human population nutrition, especially in developing countries (Broughton et al. 2003; Gepts et al. 2008; Freire-Filho et al. 2011; Boukar et al. 2016). Most *Phaseolus* and *Vigna* species have $2n = 2x = 22$ chromosomes, which are small in size (1–4 µm) and morphological similar varying from meta- to submetacentric chromosomes (Darlington and Wylie 1955; Forni-Martins 1986; Mercado-Ruaro and Delgado-Salinas 1996, 1998, 2000; Venora et al. 1999).

A BAC-FISH-based cytogenetic map was first established for *P. vulgaris* (Fonsêca et al. 2010). The established BAC markers were used for comparative mapping in *Phaseolus lunatus* L. (Bonifácio et al. 2012; Almeida and Pedrosa-Harand 2013) and *Phaseolus microcarpus* Mart. (Fonsêca and Pedrosa-Harand 2013) and revealed a generally high degree of macrosynteny among these species and collinearity breaks due to a few inversions. In turn, in the Leptostachyus group of species ($2n = 20$), the BAC markers revealed several translocations and a nested chromosome fusion that resulted in descending dysploidy (Fonsêca et al. 2016; Ferraz et al. 2020). BACs from *P. vulgaris* were also hybridized to *V. unguiculata* chromosomes and allowed identification of macrosynteny breaks involving a duplication, translocations, and inversions between species (Vasconcelos et al. 2015). Other studies included application of *V. unguiculata* BACs in genetic and physical map integration (Iwata-Otsubo et al. 2016), besides *V. unguiculata* and *P. vulgaris* BACs for BAC-FISH maps for *Vigna angularis* (Willd.) Ohwi and Ohashi (do Vale Martins et al. 2021) and *Vigna aconitifolia* (Jacq.) Maréchal (Oliveira et al. 2020). These studies enabled the expansion of the comparative cytogenetic analyses between *Vigna* and *Phaseolus* species. Although BAC-FISH is highly informative, it is a laborious process and technically challenging to identify all chromosomes in the same metaphase cells, limiting its application to a small number of species.

The availability of sequenced and assembled genomes for *V. unguiculata* (1C = 640 Mb; Lonardi et al. 2019) and *P. vulgaris* (1C = 587 Mb; Schmutz et al. 2014) allows designing oligo-FISH probes for both genomes, as previously demonstrated by oligo-painting on *Vigna* and *Phaseolus* species using probes from chromosomes 2 and 3 of *P. vulgaris* (do Vale Martins et al. 2021). Here, we present a new barcode system for the chromosome identification of both species. We compared the *V. unguiculata* and *P. vulgaris* genome sequences and selected *V. unguiculata* oligo pools from conserved regions in both species so that each chromosome is associated with a unique barcode pattern. This approach will enable comparative FISH mapping and individual chromosome identification of different *Vigna* and *Phaseolus* species and potentially other related Phaseolinae members. The accurate chromosome identification will be crucial for future investigation of chromosome evolution and diversification within the subtribe, especially for the non-model species with neither assembled genome nor available cytogenetic map.

Materials and methods

Plant material and chromosome preparation

The root tips of germinated seeds of *V. unguiculata* 'BR14 Mulato' and *P. vulgaris* 'BAT93' from Embrapa Meio-Norte (Empresa Brasileira de Pesquisa Agropecuária, Teresina, Piauí, Brazil) and Embrapa Cenargen (Embrapa Recursos Genéticos e Biotecnologia, Brasília, Distrito Federal, Brazil), respectively, were collected and pre-treated with 2 mM 8-hydroxyquinoline for 5 h at 18 °C, fixed in methanol: acetic acid (3:1 v/v) for 2–24 h at room temperature and

stored at − 20 °C until use. For chromosome preparation, the tips were washed twice in distilled water, then submitted to enzymatic treatment of 2% pectolyase (Sigma-Aldrich), 4% cellulase (Onozuka or Sigma-Aldrich), and 20% pectinase (Sigma-Aldrich) at 37 °C for 2 h in a humid chamber. The slides were prepared using the air dry technique (De Carvalho and Saraiva 1993) with minor modifications. Meristems were washed in distilled water, placed individually in an approximately 30◦ vertically inclined slide. Using a Pasteur pipette, cold fixative solution (methanol:acetic acid, 3:1, v:v) were dropped over the meristem, which were macerated until its total fragmentation. Afterward, the slides were air dried by fanning, immersed in 45% acetic acid for 5 min and placed on a hot plate surface (at 37 °C) for 5–10 min.

Selection and synthesis of Oligo-FISH probes

The Oligo-FISH barcode probes were designed using the reference genome of *V. unguiculata* 'IT97K-499-35' v. 1.1 available at Phytozome (phytozome.jgi.doe.gov) and NCBI SRA BioSample accession SAMN06674009 (also ASM 411807v1) (Lonardi et al. 2019). Unique sequences of each pseudochromosome of *V. unguiculata* were selected after filtering for excluding repetitive sequences by Arbor Biosciences (Ann Arbor, MI, USA). Probes able to generate a signal on both *V. unguiculata* and *P. vulgaris* were selected by mapping the oligo probe derived from *V. unguiculata* to the *P. vulgaris* genome (v. 2.1, http://www.phytozome.net/commonbean.php; GenBank accession ANNZ01000000; Schmutz et al. 2014) using Blastn. Only probes having a single hit in the entire *P. vulgaris* genome (Blast e-value lower than 10E-05) with this hit located on the syntenic *P. vulgaris* chromosome were retained. Two libraries were generated, which were composed of ~ 27.000 oligos each of about 45 nucleotides long. Library 1 contained the oligo pool that generated the 16 signals detected in red after FISH, while library 2 contained the second oligo pool corresponding to the 14 green signals. These libraries covered together the thirty genomic regions selected for barcoding, which corresponded to ~ 41 megabases (Mb) of DNA sequences of *V. unguiculata* genome (Data S1 and S2) and were designed and synthesized by Arbor Biosciences (Ann Arbor, MI, USA). Each library was indirectly labeled with digoxigenin (library 1) or biotin (library 2) (Han et al. 2015). The complete sequence sets of both libraries are available at Supplementary data (Data S1 and S2).

Oligo-FISH and image processing

The oligo-FISH was conducted according to the protocol proposed by Braz et al. (2020b) with some modifications. The hybridization mix consisted of 50% formamide, 2 × SSC (Saline Sodium Citrate) solution (pH 7.0), 10% dextran sulfate, 350 ng of the probe labeled with biotin-green, and 200 ng of the probe labeled in digoxigenin-red, in a total volume of 10 µL per slide. The chromosomes were denatured for 5–7 min at 75 °C and incubated for 18–72 h at 37 °C in a humid chamber. After that, the coverslips were gently removed, stringency washes in 2 × and 0.1 × SSC at 42 °C (~ 76% final stringency) were conducted, followed by a wash in 1 × TNB (Tris-NaCl-Blocking) buffer. A total of 20 µL solution comprising 0.2 µL of rhodamine sheep anti-DIG (Roche) and 0.2 µL of Alexa Fluor 488 Streptavidin (Invitrogen) was applied with posterior incubation at 37 °C for 1 h. Chromosomes were counterstained with 2 µg/mL DAPI in Vectashield antifade solution (Vector Laboratories). Chromosome images were captured with Leica DM5500B fluorescence microscope, and the adjustments for brightness and contrast of images were processed using Adobe Photoshop CC (2019). The positions of each barcode marker were measured in 20 chromatids from five metaphases per species, following Fonsêca et al. (2010), except for using the DRAWID 0.26 software (Kirov et al. 2017). The new markers were integrated into the already established maps of *V. unguiculata* (Vasconcelos et al. 2015; Oliveira et al. 2020) and *P. vulgaris* (Fonsêca et al. 2010).

In silico and integrative map analysis

The sequence set for all oligos of each barcode signal was contrasted against *V. unguiculata* 'IT97K-499-35' (ASM411807v1, GenBank ID: 8,372,728) and *P. vulgaris* 'G19833' (SAMN02981484, GenBank ID: 864,298) genomes by BLASTn tool (NCBI platform), optimized for highly similar sequences (megaBLAST), for localizing them at the pseudomolecules considering e-value, score, and identity percentage variables (Table S1). Additionally, the sequences available for BAC markers used in previous studies for both species were included. BACs from *V. unguiculata* were previously used by Oliveira et al. (2020) and do Vale Martins et al. (2021) and are available at HarvEST:cowpea (harvest.ucr.edu). The *P. vulgaris* BAC sequence accessions used for the integrated map are provided in Table S2 and were obtained by BLAST using the sequences of corresponding genetic markers used to select each BAC and provided by the studies of Vallejos et al. (1992), Murray et al. (2002), Hougaard et al. (2008), and Geffroy et al. (2009). The integrated approach was represented by circular idiograms, created with Circos software v. 0.69–9 using default parameters (Krzywinski et al. 2009), enabling an in-depth comparative analysis of the cytogenetic (outer circle) and genome (inner circle) data between *V. unguiculata* (left side) and *P. vulgaris* (right side). In order to optimize collinearity, pseudomolecules, or chromosomes were eventually inverted in orientation, being the 0 Mb their initial position, as indicated in Fig. 2. The barcode signals

are represented by continuous lines, and BAC signals are represented by dashed lines, each with 1 Mb of length. For both chromosomes and pseudomolecules, we used the species name abbreviations (*Vu* and *Pv*) followed by their chromosome numbering. Each *V. unguiculata* chromosome is represented by a different color (see Fig. 2 legend), evidencing *P. vulgaris* orthologous segments with the same colors. Output images (SVG format) were optimized using the CorelDraw X7 software.

Results

Oligo-FISH barcode development for *V. unguiculata* and *P. vulgaris* chromosome identification

FISH using two oligo probe sets, each containing 27,000 oligos, generated 16 red and 14 green signals on *V. unguiculata* metaphase chromosomes (Fig. 1a, c). Each chromosome was numbered according to the corresponding *V. unguiculata* pseudomolecules (Fig. 2). Thus, the barcode-FISH based on the cytogenetic map was fully integrated with the current genome sequence map. In *P. vulgaris* chromosomes, the two oligo-FISH probes generated 16 red signals and 13 green signals (Fig. 1b, d). The missing green signal on *P. vulgaris* is explained by the colocalization of the barcode signals 10A and 10B on *Pv*10 (Fig. 1d, f), which are separated by 3.32 Mb. *Vigna unguiculata* and *P. vulgaris* chromosomes contained one to five or four signals, respectively, which were separated by at least ~ 6.5 Mb (6.59 Mb between 4B and 4D for *Pv*4 and 7.65 Mb between 11B and 11C for *Vu*11). Except for *Vu*7, chromosomal arms without barcode signals had the presence of rDNA loci, as observed for *Vu*6, *Vu*10, *Pv*6, *Pv*9, and *Pv*10 (Fig. 2). Barcode signals covered a region from 0.19 to 1.41 Mb in length in *V. unguiculata* and from 0.03 to 4.07 Mb in *P. vulgaris* (Tables S1 and S2). Thus, it was possible to distinguish the 11 individual chromosome pairs of the two species, with each chromosome of *V. unguiculata* and *P. vulgaris* presenting a unique signal barcode pattern, which was different between species (Fig. 1).

Cytogenetic and in silico analysis: an integrated approach

In order to verify the differences in the barcode pattern between orthologous chromosomes and perform a more detailed comparison between species, the sequence set of each oligo barcode was mapped in its respective pseudomolecule. We integrated in silico and cytogenetic analyses, including the oligo-FISH barcode markers generated in this work and a set of previously developed *V. unguiculata* and *P. vulgaris* BAC-FISH markers, producing a total of 95 markers (Tables S3 and S4). Additionally, 5S and 35S rDNA sites were located in the cytogenetic maps.

We observed the same order for most markers, comparing both maps of the same species. However, we detected several discrepancies between cytogenetic and sequencing maps, including differences in chromosome sizes and morphologies, as well as distances between some markers. These discrepancies may be attributed to chromosome condensation differences between eu- and heterochromatic regions, low resolution of FISH in metaphase chromosomes, and to sequence gaps. Distortions in chromosome size were mainly observed for terminal 35S rDNA carrier chromosomes (*Vu*1, 2, 6, and 10 and *Pv*6, 9, and 10) because rDNA sites were not present at sequencing maps (Fig. 2). The lack of rDNA sites in pseudomolecules also altered the position of markers in short versus long chromosome arms in *Vu*6 and 10. To facilitate the integration of FISH and sequencing maps, chromosomes *Vu*4, 5, 6, and 10, as well as chromosome *Pv*10, were drawn in opposite orientations in relation to their respective pseudomolecules (Fig. 2).

Barcode: improvement of *V. unguiculata* and *P. vulgaris* synteny and collinearity comparisons

Based on the position of the oligo-FISH barcode markers along the chromosomes, none of the orthologous showed a conservation of the barcode pattern across the analyzed genomes (Figs. 1, 2). Chromosomes 6, 7, 9, and 11 are largely collinear, but differences in rDNA distribution between species were observed for chromosomes 6, 9, and 11.

Translocation complexes

We confirmed two translocation complexes between *V. unguiculata* and *P. vulgaris* genomes (Figs. 1, 2). Chromosomes 1, 5, and 8 were involved in a translocation complex differentiating *Vigna* and *Phaseolus* chromosomes, as previously identified by BAC-FISH, except for the participation of *Pv*5 (Vasconcelos et al. 2015; Oliveira et al. 2020; do Vale Martins et al. 2021), which was identified for the first time here by the presence of 1A in *Pv*5 and the 5A in *Pv8*. In silico analysis confirmed the rearrangements by the following oligo barcode markers: *Vu*1 short arm (*Vu*1S) (1A), *Vu*1 long arm (*Vu*1L) (1B, 1C); *Vu*5S (5B, 5C), *Vu*5L (5A); *Vu*8S (8A) and *Vu*8L (8B), which were located at *Pv*1S (8A)—*Pv*1L (1B, 1C); *Pv*5S (1A, 5B)—*Pv*5L (5C); *Pv*8S (5A)—*Pv*8L (8B) (Figs. 1, 2).

A reciprocal translocation involving chromosomes 2 and 3, previously identified by BAC-FISH analysis (Vasconcelos et al. 2015; Oliveira et al. 2020; do Vale Martins et al. 2021) and chromosome painting (do Vale Martins et al. 2021), was also detected using our barcode system. In the

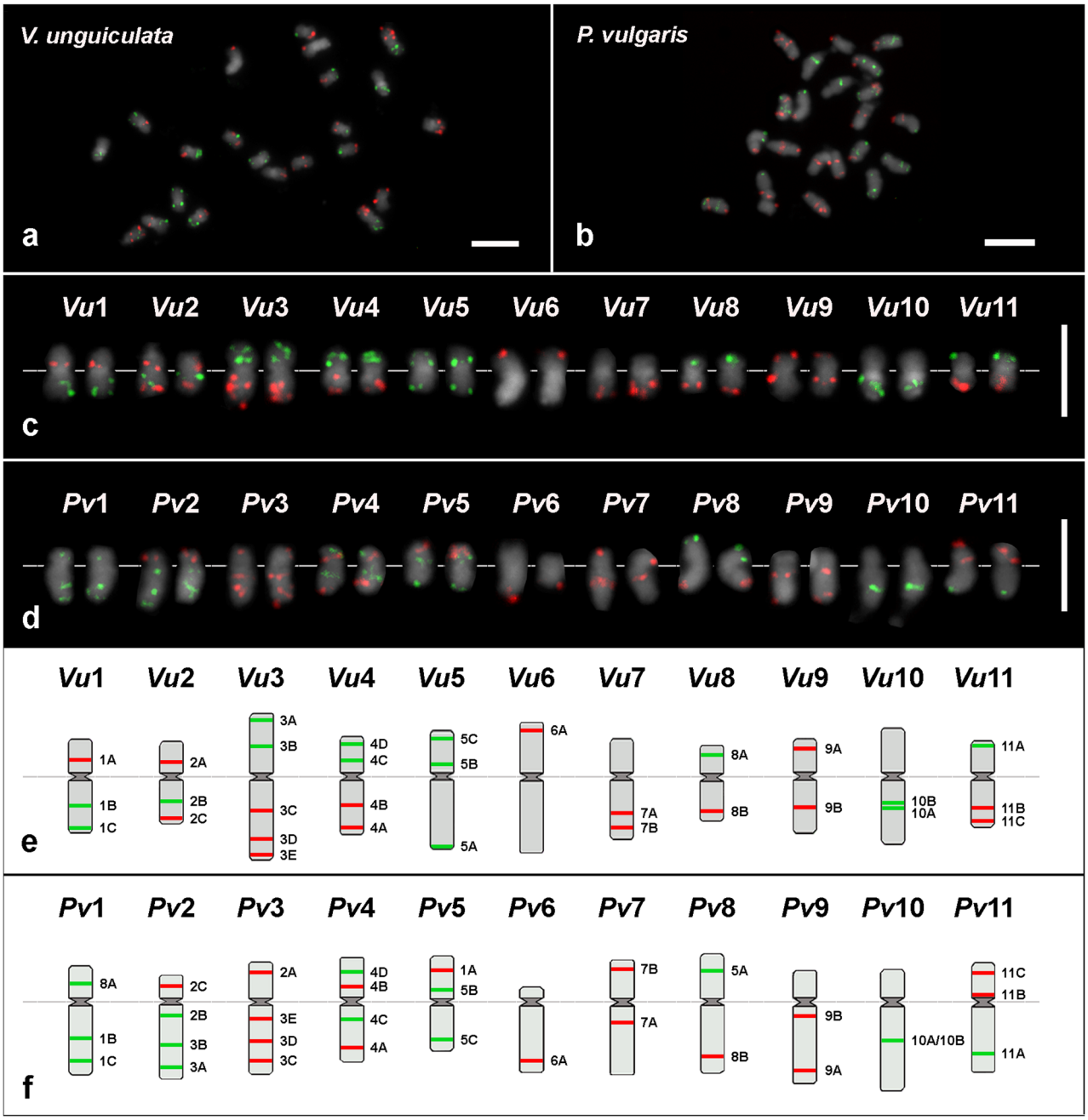

Fig. 1 Chromosome identification of *Vigna unguiculata* (*2n* = 22) and *Phaseolus vulgaris* (*2n* = 22) based on *V. unguiculata* oligo-FISH barcode. Two oligo-FISH probe sets (red and green) hybridized on mitotic metaphase chromosomes of *V. unguiculata* (**a**) and *P. vulgaris* (**b**). Homologous chromosomes in **a** and **b** were paired in karyograms to identify the 11 chromosome pairs of *V. unguiculata* (**c**) and *P. vulgaris* (**d**). Each chromosome shows a unique pattern of oligo-FISH red and/or green signals. Chromosomes were counterstained in DAPI (pseudocolored in gray). Idiograms of the barcode for both species using the *V. unguiculata* reference genome and considering the conserved sequences of *P. vulgaris* genome (**e**, *V. unguiculata* and **f**, *P. vulgaris*). Chromosomes were named according to the species name abbreviations (*Vu* and *Pv*), followed by their chromosome numbering. Each region was selected and named according to its position in *V. unguiculata* pseudomolecules starting at 0 Mb in alphabetical order. Bars in **a**–**b** = 5 µm and in **c**–**d** = 10 µm

present analysis, *Vu*2S (2A), *Vu*2L (2B, 2C); *Vu*3S (3A, 3B), and *Vu*3L (3C, 3D, 3E) markers were located at *Pv*2S (2C)—*Pv*2L (2B, 3B, 3A); *Pv*3S (2A)—*Pv*3L (3E, 3D, 3C) (Fig. 1). Additional small rearrangements, mainly involving pericentromeric regions of these two chromosomes, could be evidenced in the integrated analysis, reinforcing the centromere repositioning for chromosomes 2 and 3 described by do Vale Martins et al. (2021) (Fig. 2).

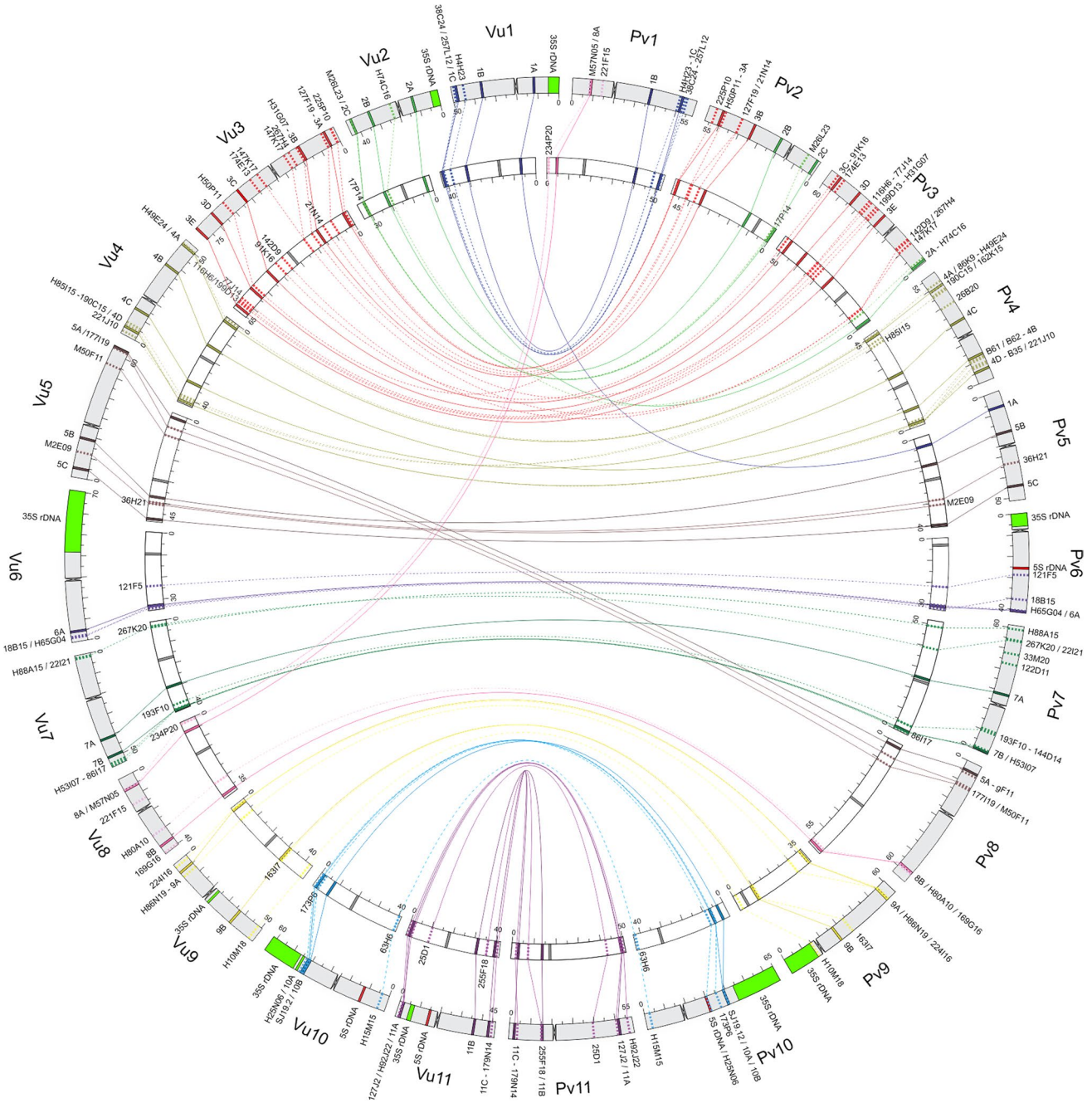

Fig. 2 Circular representation of pseudomolecules (internal) and chromosomes (external) of *Vigna unguiculata* (left side) and *Phaseolus vulgaris* (right side) showing the position of oligo barcode, BAC, and rDNA markers. Each chromosome and pseudomolecule start at 0 Mb, indicating its orientation in the present representation. Barcode markers are represented by continuous lines, while the BAC markers by dashed lines. The color of each chromosome marker was defined in accordance with *V. unguiculata* chromosomes/pseudomolecules: *Vu*1 (dark blue), *Vu*2 (light green), *Vu*3 (red), *Vu*4 (gold), *Vu*5 (brown), *Vu*6 (purple), *Vu*7 (dark green), *Vu*8 (light pink), *Vu*9 (yellow), *Vu*10 (light blue), *Vu*11 (margeta). DNAr 5S and 35S were represented by red and green, respectively. Labels of markers that colocalize are separated by "/" and of markers that are adjacent, by "-". The first label represents the marker that is closer to 0 Mb (from right to left in *Vu* and from left to right in *Pv*). The orientation of some pseudomolecules (*Pv*2, *Pv*3, *Pv*4, *Pv*7, *Pv*9, *Pv*10, and *Pv*11) and chromosomes (*Pv*2, *Pv*3, *Pv*4, *Pv*7, *Pv*9, *Pv*11, and *Vu*5) was inverted for a better visualization of synteny and collinearity

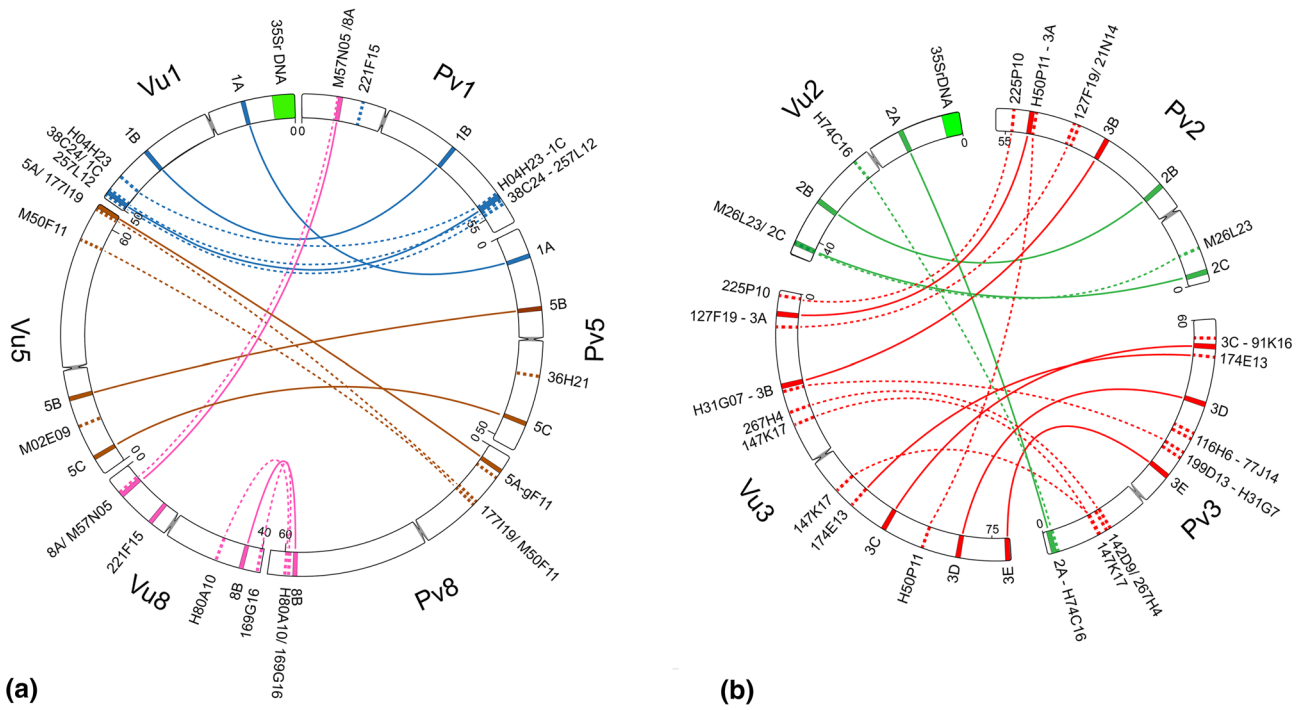

Fig. 3 Circular representation of the chromosomes 1, 5, and 8 of *Vigna unguiculata* (*Vu*) and *Phaseolus vulgaris* (*Pv*), showing the translocation complex among them (**a**), and the reciprocal translocation between chromosomes 2 and 3 (**b**), both identified using the oligo barcode and BAC probes. The measurement scale is presented in Mb. Each chromosome starts at 0 Mb, indicating its orientation in the present representation. Barcode markers are represented by continuous lines, while the BAC markers by dashed lines

Centromere repositioning of chromosomes 5, 7 and 9

In addition to the centromere repositioning for chromosomes 2 and 3 previously described (do Vale Martins et al. 2021), changes in centromere position were also detected by oligo-FISH barcode for chromosomes 5, 7, and 9 (Figs. 1, 2, 3, 4). While in *Vu*5 the centromere was positioned between 5A and 5B, in *Pv*5 it was located between 5B and 5C (Fig. 3a). For chromosome 7, the centromere was above 7A in *V. unguiculata*, while in *P. vulgaris* it was between 7A and 7B (Fig. 4a). For chromosome 9, the centromere was between 9A and 9B in *V. unguiculata* and between 9B and the distal BAC H10M18 in *P. vulgaris* (Fig. 4b).

Inversions for chromosomes 4 and 10

Apart from changes in centromere position in chromosomes 2, 3, 5, 7, and 9, the barcode markers confirmed a pericentric inversion in chromosome 4 identified by Vasconcelos et al. (2015), resulting in a barcode pattern of green–red-green–red in *Pv*4 instead of green-green–red-red in *Vu*4, and detailed the regions involved in the breakpoints (Fig. 1e–f, Fig. 5a). This was confirmed by the sequence analysis, which revealed breakpoints between 4A and BAC 190C15 in *Pv*4S, and between 4B and 4D in *Pv*4L, or the corresponding regions in *Vu*4, inverting, thus, most of the chromosome (Figs. 2, 5a). We also observed a new paracentric inversion in chromosome 10, involving the segment between H025N06 and 10B in *Pv*10L (Figs. 2, 5b). This inversion resulted in the proximity of markers 10A and 10B in *P. vulgaris*, visible as a single signal in metaphase chromosomes (Figs. 1d, f, 5b).

Discussion

A new chromosome identification system for both *V. unguiculata* and *P. vulgaris* was established in the present work. For the first time, the oligo-FISH barcode technique was used to identify legume chromosomes, by comparing sequence similarity of assembled genomes available for two species of related genera. This allowed us to design informative signal patterns for species belonging to different genera that diverged 9.7–15 Mya (Li et al. 2013; Garcia et al. 2020). We expanded the time of divergence achieved for sorghum and sugarcane (Meng et al. 2020), which diverged from a

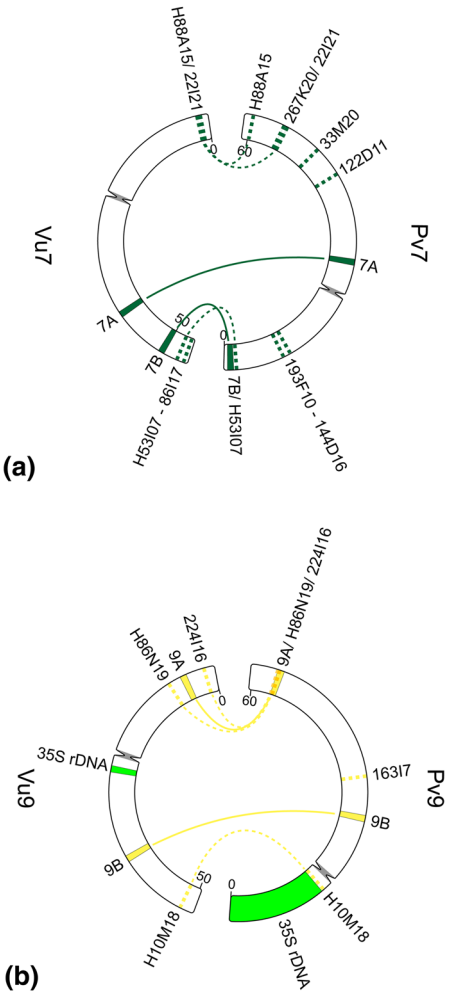

Fig. 4 Circular representation of chromosomes 7 (**a**) and 9 (**b**) of *Vigna unguiculata* (*Vu*) and *Phaseolus vulgaris* (*Pv*), both suggesting a centromere repositioning. The measurement scale is presented in Mb. Each chromosome starts at 0 Mb, indicating its orientation in the present representation. Barcode markers are represented by continuous lines, while the BAC markers by dashed lines

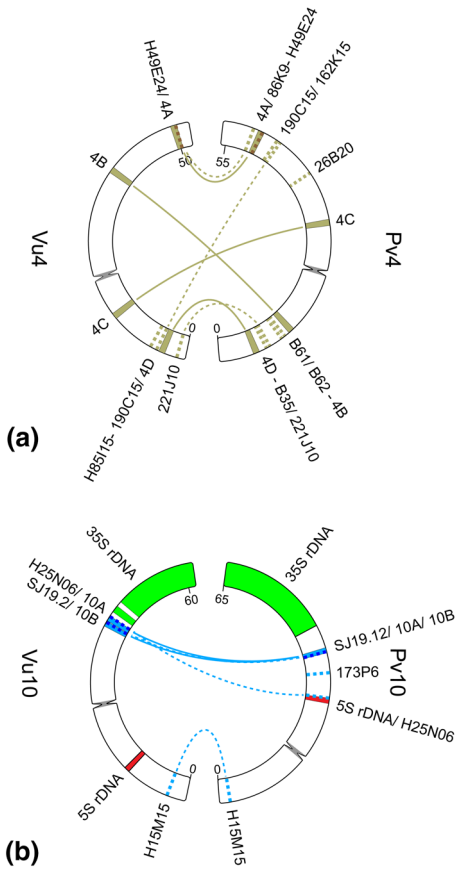

Fig. 5 Circular representation of chromosomes 4 (**a**) and 10 (**b**) of *Vigna unguiculata* (*Vu*) and *Phaseolus vulgaris* (*Pv*), evidencing a pericentric (**a**), and a paracentric (**b**) inversion, respectively. The measurement scale is presented in Mb. Each chromosome starts at 0 Mb, indicating its orientation in the present representation. Barcode markers are represented by continuous lines, while the BAC markers by dashed lines

common ancestor for 8–9 Mya (Wang et al. 2010), and similar to the time of divergence of the six Solanaceae species evaluated by Braz et al. (2018), that diverged about 15 Mya (Wu and Tanksley 2010). Our system for beans revealed new translocation complexes, inversions, and changes in centromere position involving both crop species. Oligo-FISH barcode was also used to study chromosome evolution in crops such as potato (Braz et al. 2018), rice (Liu et al. 2020), maize (Braz et al. 2020a), and sugarcane (Meng et al. 2020), identifying rearrangements as inversions, duplications and translocations.

The bean oligo-FISH barcode allowed us to identify and compare chromosomes that could not be previously analyzed cytologically, such as *Pv*5, which was identified for the first time in a translocation complex that involves chromosomes 1, 5, and 8. Furthermore, a new paracentric inversion was observed for chromosome 10, in addition to the in-depth analysis of a pericentric inversion in chromosome 4, detected cytogenetically by Vasconcelos et al. (2015). Although comparative BAC-FISH studies revealed numerous rearrangements between *V. unguiculata* and *P. vulgaris* (Vasconcelos et al. 2015; Oliveira et al. 2020), there was a lack of comparative probes for chromosome 5 and some other chromosome segments, especially in the pericentromeric region (Iwata-Otsubo et al. 2016), as observed for instance for chromosomes 4 and 10. With the establishment of the oligo-based probes, it was possible to design signals for those chromosomes and segments, including signals in more proximal positions than BACs. BAC clones may contain repetitive sequences that hinder their mapping in pericentromeric, repeat-rich chromosome regions, besides being a laborious methodology. Thus, with more genome assemblies available in the

last years, it is now possible to develop more efficient and versatile chromosome identification systems, expanding and accelerating cytogenetic analyses (Jiang 2019; Braz et al. 2020b). Vasconcelos et al. (2015) have described, for instance, a pericentric inversion for chromosome 4, using subterminal BACs from *Pv*4, while we confirmed this pericentric inversion using interstitial signals for a better characterization of the pericentromeric region of chromosome 4 of both species, narrowing down the putative breakpoint regions. Do Vale Martins et al. (2021) also reported a pericentric inversion for chromosome 4 comparing *V. unguiculata* and *V. angularis*, which belong to the subgenera *Vigna* and *Ceratotropis*, respectively, indicating that this inversion have occurred after subgenera separation (~3.6 Mya).

Although whole-genome comparison might be considered as the most complete way to shed light on chromosome evolution, most groups of plants still have only one reference genome, hampering comparative genomic analyses among closely related species (Varshney et al. 2012; Pecrix et al. 2018; Qin et al. 2019; Hasing et al. 2020). Additionally, rDNA loci and centromeres may be lacking in genome assemblies (Qin et al. 2019; Hasing et al. 2020). Our integrated cytogenetic and genomic approach highlighted the high level of macrosynteny and collinearity between both bean species (Lonardi et al. 2019). They revealed that some of the divergences in the barcode pattern between species were also related to changes in centromere position for chromosomes 2, 3, 5, 7, and 9. Centromere repositioning has been well documented in plants, such as cucumber and melon (Yang et al. 2014), maize (Schneider et al. 2016), and species of the tribe Arabideae (Brassicaceae) (Mandáková et al. 2020). Repositioning events can occur by successive peri- and paracentric inversion; intrachromosomal translocation; and/or acquisition of a new centromere (Schubert and Lysak 2011; Schubert 2018). For bean chromosomes 2 and 3, a complex rearrangement was confirmed. Besides a major translocation event, minor rearrangements were observed, such as inversions, intrachromosomal translocations, and centromere repositioning by new centromere, since collinearity was not altered between *Pv*2 and *Pv*3 pericentromeric region, as discussed by do Vale Martins et al. (2021).

For chromosomes 5, 7, and 9, centromere repositioning can be due to inversions, intrachromosomal translocation, and/or new centromere, although an association of the translocation complex involving chromosome 5 cannot be excluded. More markers are necessary to understand the involved mechanism for each of these centromeric changes. A recent study comparing *P. lunatus* (lima bean) and *P. vulgaris* genomes identified a complex intrachromosomal translocation within chromosome 9 (Garcia et al. 2020), which may be associated with the centromere repositioning observed between both species for this chromosome (Bonifácio et al. 2012). Further genome comparisons are necessary to confirm if this event also explains the difference observed between *P. vulgaris* and *V. unguiculata* chromosome 9, what, in this case, would suggest that *V. unguiculata* and *P. lunatus* chromosomes might represent the ancestral state. New centromere formation is common in domesticated plants, such as maize and potato (Talbert and Henikoff 2020), and is closely related to its domestication time (Schneider et al. 2016). This phenomenon may be associated with the selection of genes linked to the centromere. Thus, *Vigna* and *Phaseolus* beans, with multiple domestication events each, might be great targets to understand if domestication favors centromere repositioning.

Thus, the oligo-FISH barcode presented in this study provided the first legume chromosome identification enabling to distinguish individual chromosome pairs, besides identifying chromosome rearrangements and centromere repositioning not described previously. This technique can be applied to other crops of both genera that lack genomic information, such as moth bean (*V. aconitifolia*), hairy cowpea [*Vigna luteola* (Jacq.) Benth.], wild cowpea (*Vigna vexillata* L.) yearlong (*Phaseolus dumosus* Macfad.), scarlet runner (*Phaseolus coccineus* L.), and tepary bean (*Phaseolus acutifolius* A. Gray). It will probably also be useful for infrageneric comparisons of related genera, thus helping to understand the chromosome evolution of this important group of legumes.

Supplementary Information The online version contains supplementary material available at https://doi.org/10.1007/s00122-021-03921-z.

Acknowledgements We thank Embrapa Meio-Norte (Teresina, Piauí, Brazil) and Embrapa Cenargen (Brasília, Distrito Federal, Brazil) for providing the *V. unguiculata* and *P. vulgaris* seeds, respectively. We thank CNPq (Conselho Nacional de Desenvolvimento Científico e Tecnológico) Grant No. 421968/2018-4, 313527/2017-2, 310804/2017-5, 433931/2018-3, and 442019/2019-0, and FACEPE (Fundação de Amparo à Ciência e Tecnologia do Estado de Pernambuco) Grant No. APQ-0390-2.02/19 for the financial support. We also thank CAPES (Coordenação de Aperfeiçoamento de Pessoal de Nível Superior, Financial Code 001), and FACEPE for the scholarships.

Author Contribution statement FOB: designed oligo system, provided resources for the oligo-FISH experiments and wrote the paper. THN: conducted oligo-FISH experiments, analyzed the sequence synteny data, constructed Circos images and wrote the paper. CCMJ: analyzed the sequence synteny data, constructed the Circos images and helped writing the paper. SD: conducted the oligo-FISH experiments and analyzed the sequence synteny data. LVM: analyzed and processed the oligo-FISH images and helped writing the paper. GTB: labeled the oligo-FISH probes. AMBI: discussed the results. JJ: discussed the results and provided resources for the oligo probe labeling. APH: designed this research, wrote the manuscript, discussed the results and provided resources for the oligo-FISH experiments. ACBV: designed this research, the images, wrote the manuscript and discussed the results. All authors read and approved the final version of the paper.

Funding This work was supported by CNPq (Conselho Nacional de Desenvolvimento Científico e Tecnológico) Grant No. 421968/2018-4, 313527/2017-2, 310804/2017-5, 433931/2018-3, and 442019/2019-0, and FACEPE (Fundação de Amparo à Ciência e Tecnologia do Estado de Pernambuco) Grant No. APQ-0390-2.02/19.

Data availability All data generated or analyzed during this study are included as supplementary materials.

Declarations

Conflict of interest The authors declare no conflicts of interest.

References

Albert PS, Zhang T, Semrau K et al (2019) Whole-chromosome paints in maize reveal rearrangements, nuclear domains, and chromosomal relationships. Proc Natl Acad Sci 116:1679–1685. https://doi.org/10.1073/pnas.1813957116

Almeida C, Pedrosa-Harand A (2013) High macro-collinearity between lima bean (*Phaseolus lunatus* L.) and the common bean (*P. vulgaris* L.) as revealed by comparative cytogenetic mapping. Theor Appl Genet 126:1909–1916. https://doi.org/10.1007/s00122-013-2106-9

Beliveau BJ, Joyce EF, Apostolopoulos N et al (2012) Versatile design and synthesis platform for visualizing genomes with oligopaint FISH probes. Proc Natl Acad Sci 109:21301–21306. https://doi.org/10.1073/pnas.1213818110

Bi Y, Zhao Q, Yan W et al (2020) Flexible chromosome painting based on multiplex PCR of oligonucleotides and its application for comparative chromosome analyses in *Cucumis*. Plant J 102:178–186. https://doi.org/10.1111/tpj.14600

Bielski W, Książkiewicz M, Šimoníková D, Hřibová E, Susek K, Naganowska B (2020) The puzzling fate of a lupin chromosome revealed by reciprocal oligo-FISH and BAC-FISH mapping. Genes 11:1489. https://doi.org/10.3390/genes11121489

Bonifácio EM, Fonsêca A, Almeida C et al (2012) Comparative cytogenetic mapping between the lima bean (*Phaseolus lunatus L.*) and the common bean (*P. vulgaris* L.). Theor Appl Genet 124:1513–1520. https://doi.org/10.1007/s00122-012-1806-x

Boukar O, Fatokun CA, Huynh B-L et al (2016) Genomic tools in cowpea breeding programs: status and perspectives. Front Plant Sci 7:1–13. https://doi.org/10.3389/fpls.2016.00757

Braz GT, He L, Zhao H et al (2018) Comparative oligo-fish mapping: an efficient and powerful methodology to reveal karyotypic and chromosomal evolution. Genetics 208:513–523. https://doi.org/10.1534/genetics.117.300344

Braz GT, do Vale Martins L, Zhang T et al (2020a) A universal chromosome identification system for maize and wild *Zea* species. Chromosom Res 28:183–194. https://doi.org/10.1007/s10577-020-09630-5

Braz GT, Yu F, do Vale Martins L, Jiang J (2020b) Fluorescent in situ hybridization using oligonucleotide-based probes. In: Nielsen B, Jones J (eds) In situ hybridization protocols. Methods in molecular biology, vol 2148. Humana, New York, pp 71–83. https://doi.org/10.1007/978-1-0716-0623-0_4

Braz GT, Yu F, Zhao H et al (2021) Preferential meiotic chromosome pairing among homologous chromosomes with cryptic sequence variation in tetraploid maize. New Phytol 229:3294–3302. https://doi.org/10.1111/nph.17098

Broughton WJ, Hern A et al (2003) Beans (*Phaseolus* spp.): model food legumes. Plant Soil 252:55–128

Chen L, Su D, Sun J et al (2020) Development of a set of chromosome-specific oligonucleotide markers and karyotype analysis in the Japanese morning glory *Ipomoea nil*. Sci Hortic (amsterdam) 273:109633. https://doi.org/10.1016/j.scienta.2020.109633

Darlington CD, Wylie AP (1955) Chromosome atlas of cultivated plants, 2nd edn. Chromosome atlas of flowering plants, London

De Carvalho CR, Saraiva LS (1993) An air drying technique for maize chromosomes without enzymatic maceration. Biotech Histochem 68:142–145. https://doi.org/10.3109/10520299309104684

do Vale Martins L, Yu F, Zhao H et al (2019) Meiotic crossovers characterized by haplotype-specific chromosome painting in maize. Nat Commun 10:4604. https://doi.org/10.1038/s41467-019-12646-z

do Vale Martins L, Bustamante FO, Oliveira ARS, et al (2021) BAC- and oligo-FISH mapping reveals chromosome evolution among *Vigna angularis*, *V. unguiculata* and *Phaseolus vulgaris*. Chromosoma. https://doi.org/10.1007/s00412-021-00758-9

Ferraz ME, Fonsêca A, Pedrosa-Harand A (2020) Multiple and independent rearrangements revealed by comparative cytogenetic mapping in the dysploid Leptostachyus group (*Phaseolus* L., Leguminosae). Chromosom Res 28:395–405. https://doi.org/10.1007/s10577-020-09644-z

Fonsêca A, Ferraz ME, Pedrosa-Harand A (2016) Speeding up chromosome evolution in *Phaseolus*: multiple rearrangements associated with a one-step descending dysploidy. Chromosoma 125:413–421. https://doi.org/10.1007/s00412-015-0548-3

Fonsêca A, Ferreira J, dos Santos TRB et al (2010) Cytogenetic map of common bean (*Phaseolus vulgaris* L.). Chromosom Res 18:487–502. https://doi.org/10.1007/s10577-010-9129-8

Fonsêca A, Pedrosa-Harand A (2013) Karyotype stability in the genus *Phaseolus* evidenced by the comparative mapping of the wild species *Phaseolus microcarpus*. Genome 56:335–343. https://doi.org/10.1139/gen-2013-0025

Forni-Martins ER (1986) New chromosome number in the genus *Vigna* Savi (Leguminosae-Papilionoideae). Bull Du Jard Bot Natl Belgique/Bull Van Natl Plantentuin Van België 56:129. https://doi.org/10.2307/3667759

Filho FRF, Ribeiro VQ, de Rocha MM et al (2011) Feijão-Caupi no Brasil, 1st edn. EMBRAPA Meio-Norte, Teresina

Garcia T, Duitama J, Zullo S et al (2020) Comprehensive genomic resources related to domestication and crop improvement traits in Lima bean. Nat Res. https://doi.org/10.1038/s41467-021-20921-1

Geffroy V, Macadré C, David P et al (2009) Molecular analysis of a large subtelomeric nucleotide-binding-site–leucine-rich-repeat family in two representative genotypes of the major gene pools of *Phaseolus vulgaris*. Genetics 181:405–419. https://doi.org/10.1534/genetics.108.093583

Gepts P, Aragão FJL, de Barros E et al (2008) Genomics of *Phaseolus* beans, a major source of dietary protein and micronutrients in the tropics. In: Moore PH, Ming R (eds) Genomics of tropical crop plants. Springer, New York, pp 113–143

Han Y, Zhang T, Thammapichai P et al (2015) Chromosome-specific painting in *Cucumis* species using bulked oligonucleotides. Genetics 200:771–779. https://doi.org/10.1534/genetics.115.177642

Hasing T, Tang H, Brym M et al (2020) A phased *Vanilla planifolia* genome enables genetic improvement of flavour and production. Nat Food 1:811–819. https://doi.org/10.1038/s43016-020-00197-2

He L, Braz GT, Torres GA, Jiang J (2018) Chromosome painting in meiosis reveals pairing of specific chromosomes in polyploid *Solanum* species. Chromosoma 127:505–513. https://doi.org/10.1007/s00412-018-0682-9

He L, Zhao H, He J et al (2020) Extraordinarily conserved chromosomal synteny of *Citrus* species revealed by chromosome-specific painting. Plant J 103:2225–2235. https://doi.org/10.1111/tpj.14894

Hou L, Xu M, Zhang T et al (2018) Chromosome painting and its applications in cultivated and wild rice. BMC Plant Biol 18:110. https://doi.org/10.1186/s12870-018-1325-2

Hougaard BK, Madsen LH, Sandal N et al (2008) Legume anchor markers link syntenic regions between Phaseolus vulgaris, Lotus japonicus, Medicago truncatula and Arachis. Genetics 179:2299–2312. https://doi.org/10.1534/genetics.108.090084

Iwata-Otsubo A, Radke B, Findley S et al (2016) Fluorescence *in situ* hybridization (FISH)-based karyotyping reveals rapid evolution of centromeric and subtelomeric repeats in common bean (*Phaseolus vulgaris*) and relatives. G3 Genes Gen Genet 6:1013–1022. https://doi.org/10.1534/g3.115.024984

Jiang J (2019) Fluorescence *in situ* hybridization in plants: recent developments and future applications. Chromosom Res 27:153–165. https://doi.org/10.1007/s10577-019-09607-z

Jiang J, Gill BS (1994) Nonisotopic *in situ* hybridization and plant genome mapping: the first 10 years. Genome 37:717–725. https://doi.org/10.1139/g94-102

Jiang J, Gill BS (2006) Current status and the future of fluorescence *in situ* hybridization (FISH) in plant genome research. Genome 49:1057–1068. https://doi.org/10.1139/g06-076

Kirov I, Khrustaleva L, Van Laere K et al (2017) DRAWID: user-friendly java software for chromosome measurements and idiogram drawing. Comp Cytogenet 11:747–757. https://doi.org/10.3897/compcytogen.v11i4.20830

Krzywinski M, Schein J, Birol I et al (2009) Circos: an information aesthetic for comparative genomics. Genome Res 19:1639–1645. https://doi.org/10.1101/gr.092759.109

Langer-Safer PR, Levine M, Ward DC (1982) Immunological method for mapping genes on *Drosophila* polytene chromosomes. Proc Natl Acad Sci 79:4381–4385. https://doi.org/10.1073/pnas.79.14.4381

Li H, Wang W, Lin L et al (2013) Diversification of the phaseoloid legumes: effects of climate change, range expansion and habit shift. Front Plant Sci 4:1–9. https://doi.org/10.3389/fpls.2013.00386

Li G, Zhang T, Yu Z et al (2020) An efficient Oligo-FISH painting system for revealing chromosome rearrangements and polyploidization in Triticeae. Plant J 105:978–993. https://doi.org/10.1111/tpj.15081

Liu X, Sun S, Wu Y et al (2020) Dual-color oligo-FISH can reveal chromosomal variations and evolution in *Oryza* species. Plant J 101:112–121. https://doi.org/10.1111/tpj.14522

Lonardi S, Muñoz-Amatriaín M, Liang Q et al (2019) The genome of cowpea (*Vigna unguiculata* [L.] Walp.). Plant J 98:767–782. https://doi.org/10.1111/tpj.14349

Mandáková T, Hloušková P, Koch MA, Lysak MA (2020) Genome evolution in Arabideae was marked by frequent centromere repositioning. Plant Cell 32:650–665. https://doi.org/10.1105/tpc.19.00557

Meng Z, Zhang Z, Yan T et al (2018) Comprehensively characterizing the cytological features of *Saccharum spontaneum* by the development of a complete set of chromosome-specific oligo probes. Front Plant Sci 9:1–11. https://doi.org/10.3389/fpls.2018.01624

Meng Z, Han J, Lin Y et al (2020) Characterization of a *Saccharum spontaneum* with a basic chromosome number of $x = 10$ provides new insights on genome evolution in genus *Saccharum*. Theor Appl Genet 133:187–199. https://doi.org/10.1007/s00122-019-03450-w

Mercado-Ruaro P, Delgado-Salinas A (1996) Karyological studies in several Mexican species of *Phaseolus* L. and *Vigna* Savi (Phaseolinae, Fabaceae). In: Pickergill B, Lock JM (eds) Advances in legume systematics 8, Legumes of economic importance. Royal Botanic Gardens, Kew, pp 83–87

Mercado-Ruaro P, Delgado-Salinas A (1998) Karyotypic studies on species of *Phaseolus* (Fabaceae: Phaseolinae). Am J Bot 85:1–9. https://doi.org/10.2307/2446547

Mercado-Ruaro P, Delgado-Salinas A (2000) Cytogenetic studies in *Phaseolus* L. (Fabaceae). Genet Mol Biol 23:985–987. https://doi.org/10.1590/S1415-47572000000400043

Murray J, Larsen J, Michaels TE et al (2002) Identification of putative genes in bean (*Phaseolus vulgaris*) genomic (Bng) RFLP clones and their conversion to STSs. Genome 45:1013–1024. https://doi.org/10.1139/g02-069

Oliveira ARS, do Vale Martins LV, Bustamante FDO et al (2020) Breaks of macrosynteny and collinearity among moth bean (*Vigna aconitifolia*), cowpea (*V. unguiculata*), and common bean (*Phaseolus vulgaris*). Chromosom Res. https://doi.org/10.1007/s10577-020-09635-0

Pecrix Y, Staton SE, Sallet E et al (2018) Whole-genome landscape of *Medicago truncatula* symbiotic genes. Nat Plants 4:1017–1025. https://doi.org/10.1038/s41477-018-0286-7

Piperidis N, D'Hont A (2020) Sugarcane genome architecture decrypted with chromosome-specific oligo probes. Plant J 103:2039–2051. https://doi.org/10.1111/tpj.14881

Qin S, Wu L, Wei K et al (2019) A draft genome for *Spatholobus suberectus*. Sci Data 6:1–9. https://doi.org/10.1038/s41597-019-0110-x

Qu M, Li K, Han Y et al (2017) Integrated karyotyping of woodland strawberry (*Fragaria vesca*) with oligopaint FISH probes. Cytogenet Genome Res 153:158–164. https://doi.org/10.1159/000485283

Schneider KL, Xie Z, Wolfgruber TK, Presting GG (2016) Inbreeding drives maize centromere evolution. Proc Natl Acad Sci 113:E987–E996. https://doi.org/10.1073/pnas.1522008113

Schmutz J, McClean PE, Mamidi S et al (2014) A reference genome for common bean and genome-wide analysis of dual domestications. Nat Genet 46:707–713. https://doi.org/10.1038/ng.3008

Schubert I (2018) What is behind "centromere repositioning"? Chromosoma 127:229–234. https://doi.org/10.1007/s00412-018-0672-y

Schubert I, Lysak MA (2011) Interpretation of karyotype evolution should consider chromosome structural constraints. Trends Genet 27:207–216

Šimoníková D, Němečková A, Karafiátová M et al (2019) Chromosome painting facilitates anchoring reference genome sequence to chromosomes *in situ* and integrated karyotyping in banana (*Musa* spp.). Front Plant Sci 10:1–12. https://doi.org/10.3389/fpls.2019.01503

Song X, Song R, Zhou J et al (2020) Development and application of oligonucleotide-based chromosome painting for chromosome 4D of *Triticum aestivum* L. Chromosom Res 28:171–182. https://doi.org/10.1007/s10577-020-09627-0

Talbert PB, Henikoff S (2020) What makes a centromere? Exp Cell Res 389:111895. https://doi.org/10.1016/j.yexcr.2020.111895

Vallejos CE, Sakiyama NS, Chase CD (1992) A molecular marker-based linkage map of *Phaseolus vulgaris* L. Genetics 131:733–740

Varshney RK, Chen W, Li Y et al (2012) Draft genome sequence of pigeonpea (*Cajanus cajan*), an orphan legume crop of resource-poor farmers. Nat Biotechnol 30:83–89. https://doi.org/10.1038/nbt.2022

Vasconcelos EV, de Andrade Fonsêca AF, Pedrosa-Harand A et al (2015) Intra- and interchromosomal rearrangements between cowpea [*Vigna unguiculata* (L.) Walp.] and common bean (*Phaseolus vulgaris* L.) revealed by BAC-FISH. Chromosom Res 23:253–266. https://doi.org/10.1007/s10577-014-9464-2

Venora G, Blangifortil S, Cremonini R (1999) Karyotype analysis of twelve species belonging to genus *Vigna*. Cytologia (tokyo) 64:117–127. https://doi.org/10.1508/cytologia.64.117

Wang J, Roe B, Macmil S et al (2010) Microcollinearity between autopolyploid sugarcane and diploid sorghum genomes. BMC Genomics 11:261. https://doi.org/10.1186/1471-2164-11-261

Wu F, Tanksley SD (2010) Chromosomal evolution in the plant family Solanaceae. BMC Genomics 11:182. https://doi.org/10.1186/1471-2164-11-182

Xin H, Zhang T, Han Y et al (2018) Chromosome painting and comparative physical mapping of the sex chromosomes in *Populus tomentosa* and *Populus deltoides*. Chromosoma 127:313–321. https://doi.org/10.1007/s00412-018-0664-y

Yang L, Koo D-H, Li D et al (2014) Next-generation sequencing, FISH mapping and synteny-based modeling reveal mechanisms of decreasing dysploidy in *Cucumis*. Plant J 77:16–30. https://doi.org/10.1111/tpj.12355

Zhao Q, Wang Y, Bi Y et al (2019) Oligo-painting and GISH reveal meiotic chromosome biases and increased meiotic stability in synthetic allotetraploid *Cucumis* ×*hytivus* with dysploid parental karyotypes. BMC Plant Biol 19:471. https://doi.org/10.1186/s12870-019-2060-z